ACES Asian Chemical Editorial Society

DOI: 10.1002/asia.201601340

CHEMISTRY AN ASIAN JOURNAL Full Paper

Substituent Effects

Excited State Intramolecular #ProtonTransfer in Regioisomers of HBT: Effects of the Position and Electronic Nature of Substituents

Qin Wang, Longfei Xu, Yahui Niu, Yuxiu Wang, Mao-Sen Yuan,* and Yanrong Zhang*[a]

Abstract: Although the organic dyes based on excited state intramolecular proton transfer (ESIPT) mechanism have attracted significant attention, the structure-property relationship of ESIPT dyes needs to be further exploited. In this paper, three series of ethynyl-extended regioisomers of 2-(2′-hydroxyphenyl)benzothiazole (HBT), at the 3′-, 4′- and 6-positions, respectively, have been synthesized. Changes in the absorption and emission spectra were correlated with the position and electronic nature of the substituent groups. Although 4′- and 6-substituted HBT derivatives exhibited absorption bands at longer wavelengths, the keto-emission of 3′-substituted HBT derivatives was found at a substantially longer wavelength. The gradual red-shifted fluorescence emission was found for 3′-substituted HBT derivatives where the electron-donating nature of substituent group increased, which was opposite to what was observed for 4′- and 6-substituted HBT derivatives. The results derived from the theoretical calculations were in conformity with the experimental observations. Our study could potentially provide experimental and theoretical basis for designing novel ESIPT dyes that possess unique fluorescent properties.

Introduction

Proton-transfer reactions play very important roles in many chemical and biological processes.[1] The excited state intramolecular proton transfer (ESIPT) process refers to a photoinduced tautomerization of the enolform to the ketoform in the excited state through a pre-existing intramolecular hydrogen bond in the subpicosecond time scale,[2–7] followed by a relaxation of the excited keto tautomer to its ground state accompanied by fluorescence emission. It subsequently returned to its energetically favored ground-state enol tautomer via ground state intramolecular proton transfer (GSIPT).[8–10] Because of the significant difference between the absorbing species (enol tautomer) and the emitting species (keto tautomer) in terms of structure and electronic configuration, ESIPT fluorophores usually exhibit fluorescence emission with larger Stokes shifts than common fluorophores.[11–13]

2-(2′-Hydroxyphenyl)benzothiazole (HBT), a typical ESIPT dye, has been extensively studied experimentally and theoretically due to its structural simplicity, facile preparation and chemical stability.[13–17] Chemical modifications of the existing ESIPT dyes are often efficient strategies to precisely control ESIPT and to meet specific applications. Wang et al. modified the 4′- and 5′-positions of HBT with tertiary amino groups, and studied the electronic effects of different electron-donating amino groups on the photophysical properties.[18] However, they did not synthesize any other regioisomers of amino HBT derivatives and their synthetic strategy has not yet been conveniently exploited to introduce other substituents. Han et al. introduced an electron-donating group (triphenylamine) in the 6-position and an electron-withdrawing group (trifluoromethyl) in the 4′-position simultaneously, to obtain an HBT derivative, which can generate pure white light emission in mixed solvents.[19] Zhao et al. conjugated the naphthalimide at the 5′-position of HBT through C≡C linker and observed a long-lived triplet state for this HBT derivative.[20] Zhao et al. also reported another HBT derivative with a boron-dipyrromethene substituent in the 5′-positon, which showed no ESIPT effect.[21] These studies demonstrated that subtle structural changes on HBT might bring about dramatic impact on its photophysical properties. Despite the potential practical application of the HBT derivatives,[22–26] the structure-property relationship of the ESIPT dyes is still obscure and needs to be further exploited. Establishing this relationship could provide experimental and theoretical guidance to meet specific applications through further chemical transformations.

Herein, it is aimed to develop a facile method to synthesize three series of ethynyl-extended regioisomers of HBT, at the 3′-, 4′- and 6-positions, respectively (molecular structures shown in Scheme 1), and to study the influence of the position and electronic nature of substituents on the ESIPT process by using steady-state fluorescence in different solvents as well as theoretical calculations.

[a] Dr. Q. Wang, Dr. L. Xu, Dr. Y. Niu, Dr. Y. Wang, Dr. M.-S. Yuan, Dr. Y. Zhang
College of Science
Northwest A&F University
Yangling, Shaanxi 712100 (P. R. China)
E-mail: yuanms@nwsuaf.edu.cn
zhangyr@nwsuaf.edu.cn

Supporting information for this article can be found under http://dx.doi.org/10.1002/asia.201601340.

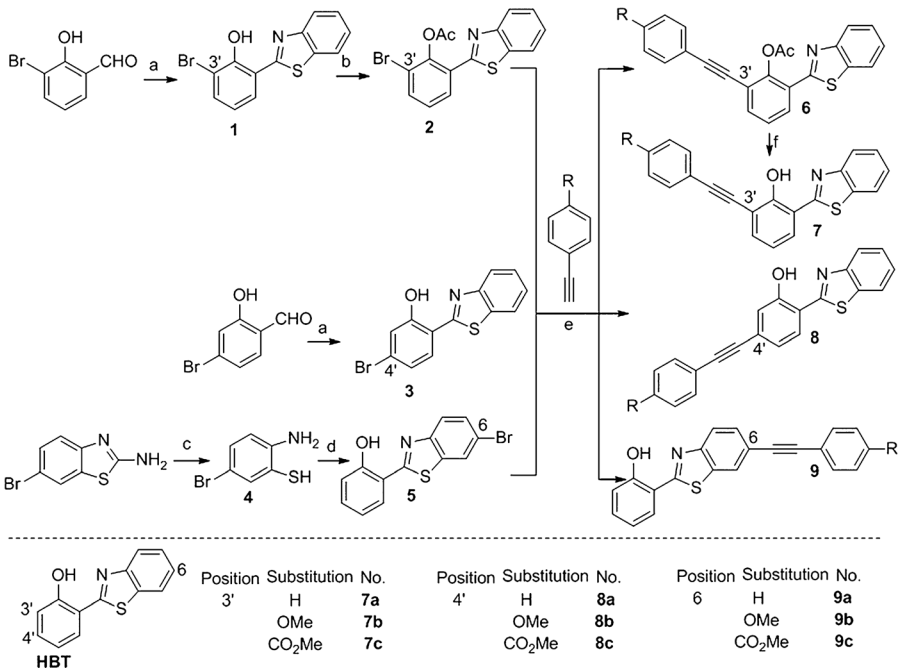

Scheme 1. Synthetic routes and molecular structures of ethynyl-extended regioisomers of HBT. (a) 2-aminothiophenol, C_2H_5OH, H_2O_2, HCl, RT, 0.5 h; (b) Ac_2O, pyridine, CH_2Cl_2, RT; (c) KOH, H_2O, reflux; (d) salicylaldehyde, C_2H_5OH, H_2O_2, HCl, RT, 0.5 h; (e) $PdCl_2(PPh_3)_2$, CuI, NEt_3, Toluene, nitrogen atmosphere, 90 °C, 12 h; (f) K_2CO_3, MeOH/THF, RT.

Results and Discussion

Design and synthesis of ethynyl-extended regioisomers of HBT

Various groups with different Hammett substituent constants (σ) were introduced via Sonogashira cross-coupling reactions between terminal alkynes and aryl halides.[27–29] The commercially available regioisomers of brominated salicylaldehyde could make further chemical modification feasible. Synthetic strategies of the 3′-, 4′- and 6-substituted regioisomers of HBT are outlined in Scheme 1. Reaction between 3-bromosalicylaldehyde or 4-bromosalicylaldehyde and 2-aminothiophenol in the presence of HCl/H_2O_2 in methanol yielded 3′- and 4′-bromo-substituted HBT **1** or **3**, which could be readily monitored by thin layer chromatography (strong yellow color). When the aryl halide has a nucleophilic substituent group (e.g., OH) in the *ortho* position, cyclization to the corresponding heterocyclic compound occurs exclusively under Sonogashira reaction conditions.[30,31] Therefore, **1** was protected using acetic anhydride in a large excess of pyridine to provide **2**. After workup, the crude reaction mixture was directly subjected to Sonogashira cross-coupling conditions (Pd^{II}, CuI, NEt_3, toluene),[31] with aromatic acetylenes to yield acetate-protected HBT **6**. By removing the acetate protecting group under alkaline condition (K_2CO_3, MeOH/THF), the target 3′-substituted HBT derivatives **7** were obtained. Under the same Sonogashira cross-coupling conditions, 4′-bromo-substituted HBT derivative **3** reacted directly with aromatic acetylenes to yield 4′-substituted HBT derivatives **8**.

We have chosen commercially available 2-amino-6-bromobenzothiazole as the starting material to synthesize 6-substituted HBT derivatives **9**. 2-Amino-6-bromobenzothiazole was hydrolyzed under strong alkaline condition to provide 5-bromo-2-aminothiophenol **4**.[32] 6-Bromo-substituted HBT **5** was obtained by reacting **4** with salicylaldehyde in the presence of HCl/H_2O_2, in methanol. Under Sonogashira conditions, 6-substituted HBT derivatives **9a**, **9b** and **9c** were obtained. These new compounds were unambiguously characterized by NMR spectroscopy and HRMS (Supporting Information, Figures S18–S48). Single-crystal X-ray analysis was also performed for **8a** (Figure 1), which further confirmed the connection of the phenylacetylene fragment at the 4′-position of HBT and clearly revealed the presence of an intramolecular hydrogen bond between the hydroxyl proton and the nitrogen atom of benzothiazole moiety (1.900 Å). Suitable crystals of other compounds could not be obtained.

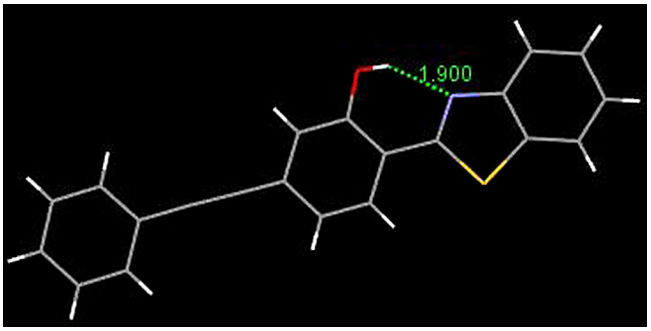

Figure 1. Crystal structure of 4′-substituted HBT derivative **8a**.

The effect of substituent position on the fluorescence spectra of HBT derivatives

In order to study the photophysical properties of ethynyl-extended regioisomers of HBT derivatives bearing the same substituent group at the 3′-, 4′- or 6-position of HBT, we have compared the absorption and fluorescence emission spectra of phenylethynyl-substituted HBT derivatives (**7a**, **8a** and **9a**), 4-methoxyphenylethynyl-substituted HBT derivatives (**7b**, **8b** and **9b**) and 4-methylbenzoate ethenyl-substituted HBT derivatives (**7c**, **8c** and **9c**) in toluene. Previous studies have revealed that the existence of a stable intramolecular H-bond between the phenolic hydroxyl proton and nitrogen atom in the benzothiazole ring is a prerequisite for the proton transfer from the O atom to the N atom to occur, in order to complete the tautomerization from enol to keto form at excited state.[33] The non-H-bonding non-polar solvents cannot interfere with the H-bond between the N atom of the benzothiazole ring and the phenolic hydroxyl proton, the closed *cis*-enol form being the most stable conformer for these dyes. This conformer undergoes ESIPT upon excitation to form the keto tautomer and gives rise to keto emission, as shown in Scheme 2.[34]

Figure 2 depicts the steady-state absorption and fluorescence emission spectra of the examined HBT derivatives in toluene. The fluorescence excitation spectra of these compounds (Figure S1, Supporting Information) closely correspond to their respective absorption spectrum, which indicate that the keto emission originated from the group state absorbing species.[25,35] The photophysical data of these three series of HBT derivatives including their maximum absorption wavelength (λ_{abs}), maximum emission wavelength (λ_{em}), molar extinction coefficient (ε_{max}), Stokes shift values ($\Delta\lambda$) and fluorescence quantum yields (Φ_f), are summarized in Table 1. 3′-Substituted HBT derivatives (**7a**, **8a** and **9a**) have λ_{abs} values of 358 nm, 374 nm and 371 nm, respectively (Figure 2a), and λ_{em} values of 551 nm, 522 nm and 522 nm, respectively (Figure 2b). In comparison with the parent compound HBT (λ_{abs} = 347 nm, λ_{em} = 516 nm) (Figure S2), compounds **7a**, **8a** and **9a** exhibit absorption bands and emit fluorescence from the excited keto-tautomer K* at longer wavelengths, which indicates that the introduction of an aromatic ethynyl moiety indeed enlarges the π-conjugation and decreases the energy gap between the ground and excited states of the keto-tautomer, regardless of the connected positions. In the absorption spectra (Figure 2a), the magnitude of bathochromic shift is much higher for 4′- (27 nm) and 6-substituted (24 nm) HBT derivatives **8a** and **9a**than that of 3′-substituted HBT derivative **7a** (11 nm). Moreover, the ε_{max} value is also much higher for 4′- (2.85×10^4 M^{-1}cm^{-1}) and 6-substituted (3.48×10^4 M^{-1}cm^{-1}) HBT derivatives **8a** and **9a** than for 3′-substituted HBT derivative **7a** (1.57×10^4 M^{-1}cm^{-1}). The difference in λ_{abs} and ε_{max} values might be associated with the different planarity of the dyes, since less planar molecular structures usually show a lower probability for the π–π* transition.[36,37] However, in the fluorescence emission spectrum (Figure 2b), the red-shifted magnitude for 3′-substituted HBT **7a** (35 nm) is much higher than that of 4′- and 6-substituted HBT derivatives **8a** and **9a** (5 nm).

Table 1. Steady-state photophysical properties of the ethynyl-extended regioisomers of HBT in toluene solution.

	7a	8a	9a	7b	8b	9b	7c	8c	9c
λ_{abs}[a] [nm]	358	374	371	364	382	379	361	378	379
λ_{em}[b] [nm]	551	522	522	557	520	520	549	524	525
$\varepsilon_{max}\times10^4$[c] [M^{-1}cm^{-1}]	1.57	2.85	3.48	1.74	3.78	3.52	2.18	3.41	3.75
$\Delta\lambda$[d] [nm]	193	148	151	193	138	141	188	146	146

[a] The maximum absorption wavelength; [b] The maximum fluorescence emission wavelength; [c] The molar absorption coefficient; [d] Strokes shift.

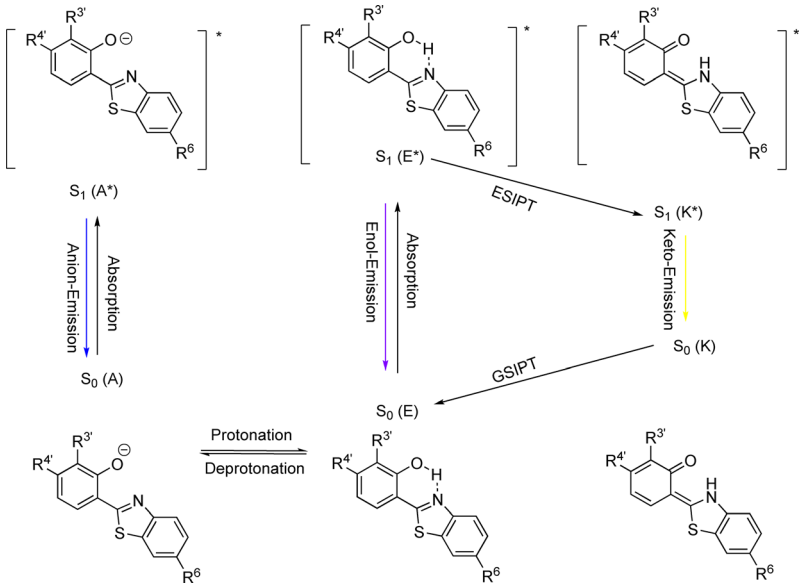

Scheme 2. Schematic representation of the photophysical process for the ethynyl-extended regioisomers of HBT.

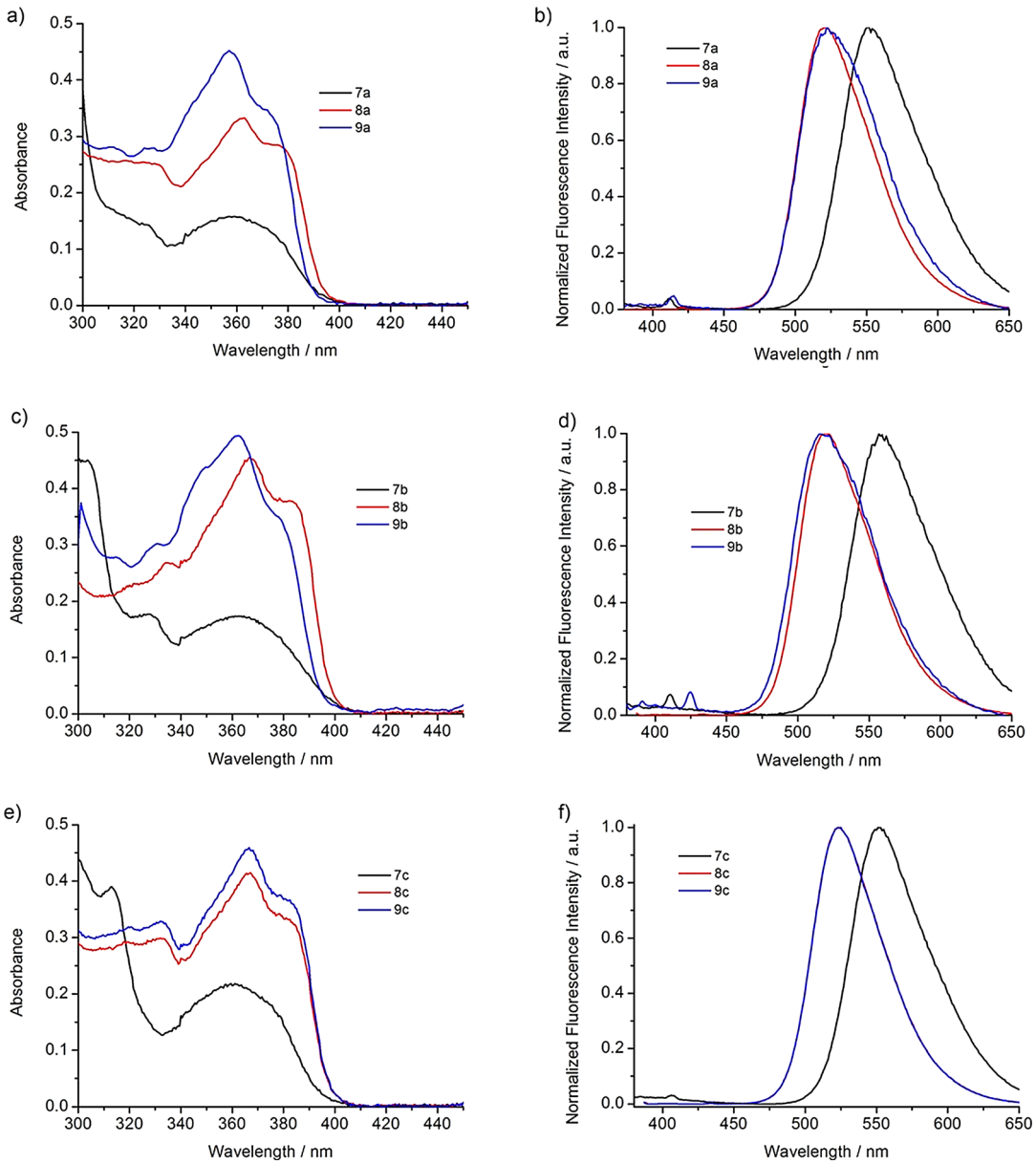

Figure 2. The absorption and emission spectra of ethynyl-extended regioisomers of HBT in toluene solution. The top row for phenylethynyl modified HBT derivatives (**7a**, **8a** and **9a**), the middle row for 4-methoxyphenylethynyl-substituted HBT derivatives (**7b**, **8b** and **9b**), and the bottom row for 4-methylbenzoateethyny-substituted HBT derivatives (**7c**, **8c** and **9c**).

Therefore, the Stokes shift with respect to the absorption peak wavelength for 3′-substituted HBT derivative **7a** (193 nm) is larger than those of 4′- and 6-substituted HBT derivatives **8a** and **9a** (148 and 151 nm, respectively), these large Stokes shifts also supporting the occurrence of the ESIPT process. A similar trend was also observed for 4-methoxyphenylethynyl-substituted regioisomers of HBT **7b**, **8b** and **9b** (Figures 2c–2d), as well as for 4-methylbenzoate ethenyl-substituted regioisomers of HBT **7c**, **8c** and **9c** (Figures 2e–2f). Therefore, it could be concluded that the 3′-position of HBT is preferred for designing ESIPT fluorescent compounds that are capable of possessing red-shifted emission spectra.

The electronic effect of substituent groups on the fluorescence spectra of HBT derivatives

In the previous section, the position effect of the substituent on the fluorescence spectra of HBT derivatives has been explored. In this section, we examined the electronic effect of substituents connected at the different positions of HBT on the fluorescent spectra. All fluorescent spectra were recorded at room temperature with excitation at the maximum absorption wavelength and showed solvent-dependent behavior (see Figures 3–5). The main emission wavelengths have been summarized in Table 2. The absorption spectra recorded in different solvents resembled their corresponding excitation spectra (Fig-

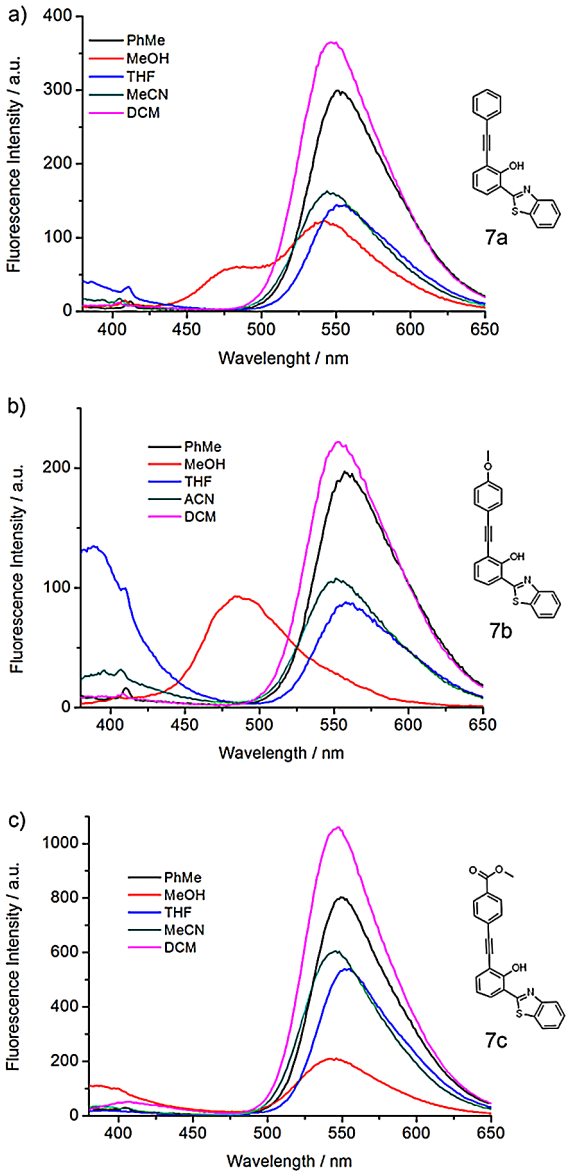

Figure 3. Fluorescence spectra of 3′-substituted HBT derivatives in various solvents. a) for **7a**, b) for **7b**, c) for **7c**.

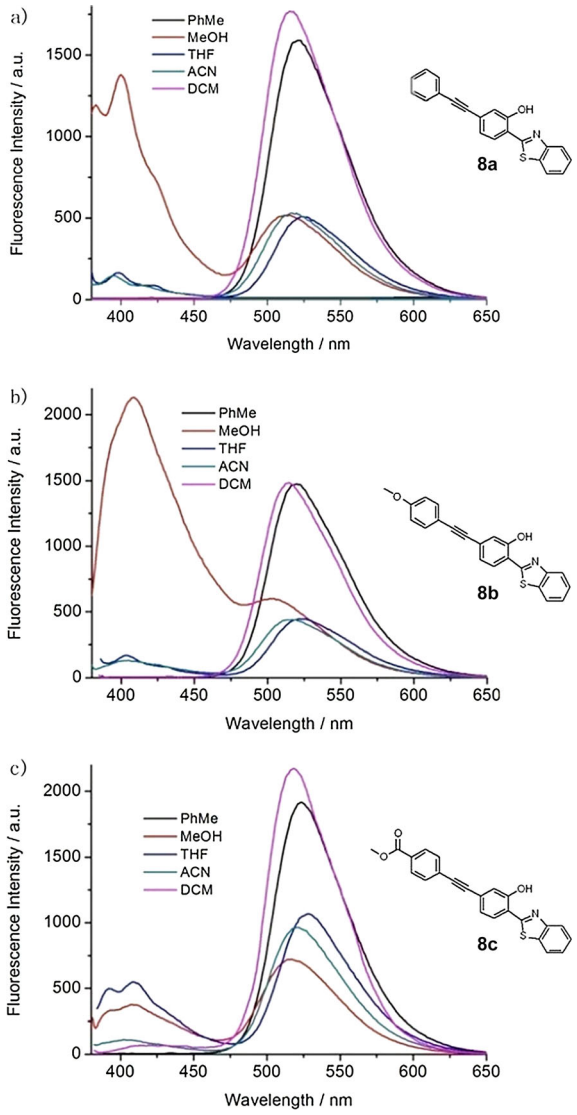

Figure 4. Fluorescence spectra of 4′-substituted HBT derivatives in various solvents. a) for **8a**, b) for **8b**, c) for **8c**.

ures S3–S11), which demonstrated that the fluorescence emission stemmed from the ground state absorbing species.[25]

The electronic effect of substituent groups on the fluorescence spectra of the 3′-substituted HBT derivatives

3′-Substituted HBT derivatives **7a**, **7b** and **7c** show only the keto emission in non-H-bonding solvents such as PhMe and

Table 2. The main emission wavelengths of ethynyl-extended regioisomers of HBT in various solvents.

Substituent group	**7a** H	**7b** OMe	**7c** CO_2Me	**8a** H	**8b** OMe	**8c** CO_2Me	**9a** H	**9b** OMe	**9c** CO_2Me
σ	0	−0.27	0.45	0	−0.27	0.45	0	−0.27	0.45
Chemical shift	13.362	13.324	13.413	12.646	12.614	12.652	12.414	12.403	12.664
Φ_f [%] in PhMe	2.69	1.40	4.27	6.40	5.67	8.67	5.96	4.43	8.20
λ_{em} [nm] in PhMe	551	557	549	522	520	524	522	520	525
λ_{em} [nm]in CH_2Cl_2	547	552	546	515	514	518	518	517	519
λ_{em} [nm] in THF	550	558	553	523	521	529	396	404	527
λ_{em} [nm] in MeCN	544	551	546	520	519	521	483	411	521
λ_{em} [nm] in MeOH	542	484	547	514	502	517	399	413	518

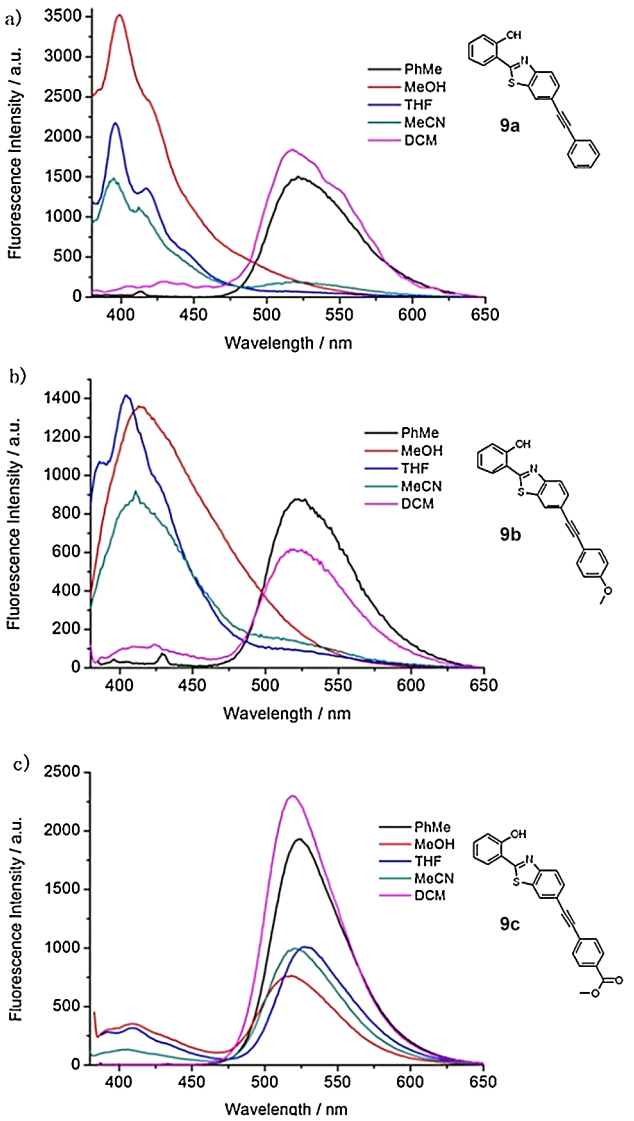

Figure 5. Fluorescence spectra of 6-substituted HBT derivatives in various solvents. a) for **9a**, b) for **9a**, c) for **9a**.

CH_2Cl_2. In comparison with **7a**, **7b** bearing the electron-donating group OMe showed a red-shifted fluorescence with a decrease in Φ_f, while **7c**, bearing the electron-withdrawing group CO_2Me showed the opposite. For example, in PhMe, the λ_{em} of **7a** is 551 nm and its Φ_f is 2.69%, while the λ_{em} of **7b** with −0.27 σ red-shifts to 557 nm and its Φ_f decreases to 1.4%; the λ_{em} of **7c** with 0.45 σ blue-shifts to 549 nm and its Φ_f increases to 4.27%. These results are consistent with our previously reported change trend for 5′-substituted HBT derivatives.[29] In THF and MeCN, which can act as H-bond acceptors, only the keto emission was detected for **7c**, while both keto and enol emission were detected for **7a** and **7b**, which is a typical characteristic of ESIPT dyes. The difference of fluorescence emission in THF and MeCN indicates that the intramolecular H-bond in the HBT derivative with smaller σ is weaker,[38] therefore, more likely to be destroyed by solvent molecules.[29] In the polar protic solvent MeOH, **7b** has emission at 484 nm, which could be assigned to anion species (A*–A, Scheme 2); **7a** shows dual emission (482 and 542 nm), which stems from anion species and keto tautomer, respectively; **7c** shows dual emission (547 and 387 nm), which originates from keto tautomer and enol tautomer, respectively. The different fluorescent spectra in MeOH further imply that the intramolecular H-bond in the HBT derivative with larger σ value is reinforced, which facilitates the ESIPT process to produce keto emission. Actually, the strength of the intramolecular H-bond can also be observed by ^{1}H NMR spectroscopy, with the chemical shift of the phenolic hydrogen proton gradually moving downfield for the HBT derivatives with large σ (Table 2 and Figures S19, S22, S25)[29,39].

The electronic effect of substituent groups on the fluorescence spectra of the 4′-substituted HBT derivatives

Similar to 3′-substituted HBT derivatives **7**, 4′-substituted HBT derivatives **8a**, **8b** and **8c** also show only the keto emission in non-H-bonding solvents such as PhMe and CH_2Cl_2. However, the change trend is different from that of the 3′-substituted HBT derivatives. In comparison with **8a**, HBT derivative **8b** bearing an electron-donating OMe group shows the blue-shifted fluorescence with a decrease in Φ_f, and the HBT derivative **8c** with the electron-withdrawing CO_2Me group shows the opposite trend. For example, in PhMe, the λ_{em} of **8a** is 522 nm and its Φ_f is 6.40%; the λ_{em} of **8b** with −0.27 σ blue-shifts to 520 nm and its Φ_f decreases to 5.67%; the λ_{em} of **8c** with 0.45 σ red-shifts to 524 nm and its Φ_f increases to 8.67%. In THF and MeCN, both keto and enol emissions are detected for all three 4′-substituted HBT derivatives. In MeOH, unlike the 3′-substituted HBT derivatives **7**, compounds **8a**, **8b** and **8c** show dual emission, originating from the keto tautomer and enol tautomer; the ratio is increasing for the 4′-substituted HBT derivative with larger σ, which also indicates that the intramolecular H-bond in the HBT derivative with larger σ is reinforced. The change in the chemical shift of the phenolic hydrogen proton can reflect the relative strength of the intramolecular H-bond of the 4′-substituted HBT derivatives (Table 2 and Figures S29, S32, S35), which are similar to the 3′-substituted HBT derivatives.

The electronic effect of substituent groups on the fluorescence spectra of the 6-substituted HBT derivatives

6-Substituted HBT derivatives **9a**, **9b** and **9c** also show only the keto emission in PhMe and CH_2Cl_2. Compared to **9a**, HBT derivative **9b**, bearing an electron-donating OMe group, shows blue-shifted fluorescence with a decrease in Φ_f, while HBT derivative **9c**, bearing the electron-withdrawing CO_2Me group, shows the opposite trend. Therefore, the electronic effect of substituent groups on the fluorescence spectra of the 6-substituted HBT derivatives is the same as that of 4′-substituted HBT derivatives, but is opposite to that of 3′-substituted HBT derivatives. For example, in PhMe, the λ_{em} of **9a** is 522 nm and its Φ_f is 5.96%; the λ_{em} of **9b** with −0.27 σ blue-shifts to 520 nm and its Φ_f decreases to 4.43%; the λ_{em} of **9c** with 0.45 σ red-shifts to 525 nm and its Φ_f increases to 8.2%. In THF and MeCN, both **9a** and **9b** show enol emission; **9c** shows dual

emission in both solvents, which could be assigned to the keto emission and enol emission, respectively. In MeOH, **9a** and **9b** emit in the enol form, while **9c** emits as both enol and keto tautomer.

Considering the fluorescent spectra of the ethynyl-extended regioisomers of HBT in various solvents together, a red-shifted keto emission could be detected when the electron-donating nature in 3′-position of HBT increased; on the other hand, the keto emission was blue-shifted when an electron-donating group at the 4′- or 6-position of HBT is introduced, manifesting an opposite electronic effect. The experimentally observed trends are well in line with the theoretical calculations (vide infra). Regardless of the connected position, increasing the electron-withdrawing nature of substituents is highly important to observe keto emission of the substituted HBT, as it could also be inferred from previous results.[40] Moreover, the conjugated substituents with large σ value on HBT can improve the Φ_f, which does not show any relationship with the connected position.[41,42] Therefore, the tunable ESIPT fluorescence could be observed by changing the electronic nature and position of substituents.

Theoretical calculation on the ethynyl-extended regioisomers of HBT

Theoretical investigations were then conducted for the enol and ketotautomers of these HBT derivatives to understand the effects of the electronic nature and position of substituents on the photophysical properties of the ethynyl-extended regioisomers of HBT in toluene.[43,44] The optimized S_0 and S_1 state geometries of the enol form of HBT derivatives **7a**, **8a** and **9a** are shown in Figure 6, while those of the other HBT

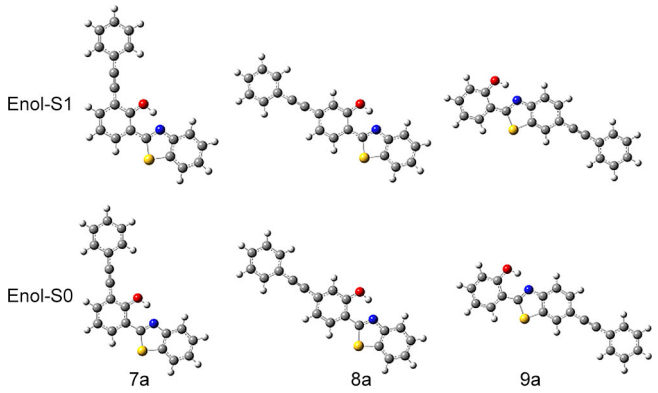

Figure 6. The energy-optimized structures of enol tautomer of phenylethynyl-substituted HBT derivatives **7a**, **8a** and **9a**. In the ball-and-stick representation, carbon, nitrogen, oxygen and sulfur atoms are colored in gray, blue, red and yellow, respectively.

derivatives are shown in Figures S12–S13. In both S_0 and S_1 states, the aryl ethynyl moiety is coplanar with the HBT part, which indicates that the aryl ethynyl moiety could indeed extend the π-conjugation of HBT and that these HBT derivatives present red-shifted absorption bands in comparison with the parent compound HBT. From S_0 to S_1 state, the bond lengths of O–H are all elongated (Tables S2–S37), which indicates that there is an increase in the acidity of the phenolic hydroxyl proton in the excited state, a prerequisite for ESIPT.[45] However, the change in magnitude for 3′-substituted HBT derivatives is very significant, ranging between of 0.0423 and 0.0593 Å, whereas the change in magnitude for 4′- and 6-substituted HBT derivatives is relatively smaller, with values of 0.0069–0.0076 Å and 0.0039–0.0089 Å, respectively. This difference between ethynyl-extended regioisomers of HBT is also supported by the change of electronic distribution from S_0 to S_1 state, which is shown in Figure 7 and Figures S14–S15. For

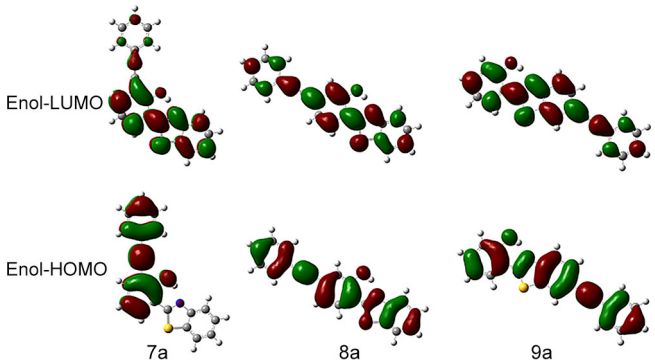

Figure 7. The calculated HOMO/LUMO and electronic contribution of enol-form of phenylethynyl-substituted HBT derivatives (**7a**, **8a** and **9a**).

3′-substituted HBT derivatives, in the S_0 state, the HOMO is located on the phenol ring and the aryl ethynyl moiety, while in the S_1 state, the LUMO is distributed on the phenol ring and the benzothiazole ring, respectively. This obvious electron migration from S_0 to S_1 state provides the prerequisites for ESIPT. However, for 4′- and 6-substituted HBT derivatives, the electrons are evenly distributed throughout the molecule in the S_0 state, but showing a slight migration toward the HBT moiety in the S_1 state. Based on the above-mentioned results, it could be concluded that the chemical modification on the 3′-position of HBT is favorable to design novel ESIPT dyes.

Theoretical results of the keto tautomers of HBT derivatives are shown in Figures 8, S16 and S17. For the 3′-substituted HBT derivatives, the HOMO and is mainly located on the phenol ring and the aryl alkynyl moiety, while the LUMO is on the phenol ring and the benzothiazole ring. Therefore, the electronic nature of the substituent influences the HOMO. For the 4′- and 6-substituted HBT derivatives, the HOMO is mainly located on the phenol ring and the benzothiazole ring, and not on the aryl alkynyl moiety; however, the electronic distribution extends to the aryl alkynyl moiety for the LUMO. Therefore, the substituent effect is more significant for the LUMO than the HOMO. According to previous reports, the σ value could be exploited to interpret the substituent effect on the emission properties.[41–43] Thus, the calculated energy levels of the HOMO and LUMO of the keto tautomers of 3′-,4′- and 6-substituted HBT were plotted as a function of σ values, as shown in Figure 9a. For HBT derivatives, regardless of the sub-

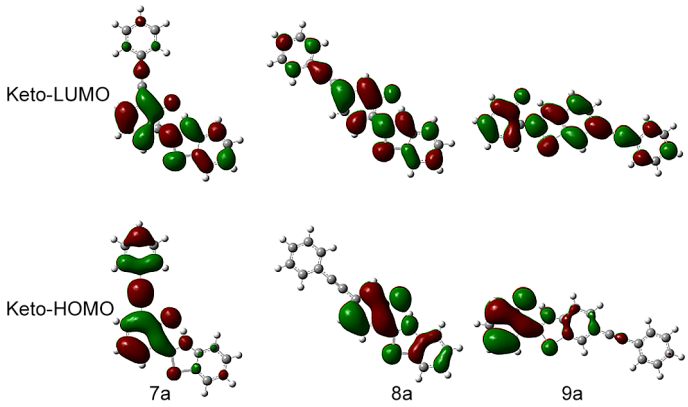

Figure 8. The calculated HOMO/LUMO and electronic contribution of keto-form of phenylethynyl-substituted HBT derivatives (**7a**, **8a** and **9a**).

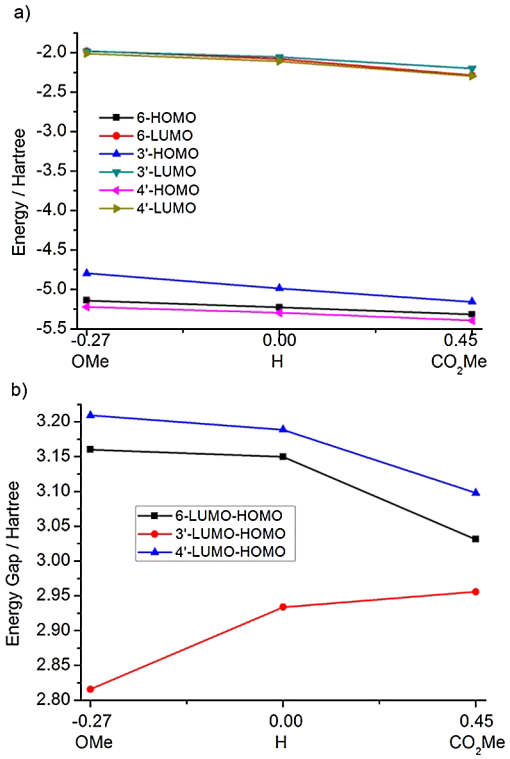

Figure 9. (a) Plot of the calculated energy levels of HOMO and LUMO of HBT derivatives against σ; (b) Plot of the calculated energy gap between HOMO and LUMO of HBT derivatives against σ.

stituted positions, the energy levels of both HOMO and LUMO decreased when the electron-donating nature of the substituent group decreased. The calculated energy gap between HOMO and LUMO of HBT derivatives against σ value is shown in Figure 9b. Adding an electron-withdrawing substituent in the 3′-position of HBT showed a decrease in energy magnitude for the HOMO, and also for the LUMO, leading to a bigger energy gap between HOMO and LUMO. The opposite effect was observed in the case of electron-donating substituents. When adding an electron-withdrawing substituent at the 4′- or 6-position, the decrease in magnitude of the energy of the LUMO was larger than that of the HOMO, resulting in a smaller energy gap between HOMO and LUMO. Again, the opposite effect was observed when electron-donating groups were present. Therefore, these theoretical calculations were consistent with the experimentally observed results.

Conclusions

Syntheses of ethynyl-extended regioisomers of HBT at its 3′-, 4′- and 6- positions were described and the effect of the position and electronic nature of substituents on their ESIPT fluorescence properties was studied. Introducing electron-donating and electron-withdrawing groups at the 3′-position of HBT led to red and blue shifts of the ESIPT fluorescence, respectively. Introducing such groups at the 4′ or 6-position of HBT resulted in fluorescence shifts in the opposite direction. Theoretical calculations demonstrated that for 3′-substituted HBT derivatives, the HOMO–LUMO energy gap became larger when the Hammett constant of substituent increased, since the HOMO was more affected by the electronic nature of substituted group. For the 4′- and 6-substituted HBT derivatives, the HOMO–LUMO energy gap became larger with decreasing Hammett constants with a more pronounced substituent effect on the LUMO. These theoretical calculations support the experimentally observed results and our study could provide an experimental and theoretical basis for the chemical modification on the ESIPT dyes that possess unique fluorescent properties.

Experimental Section

Materials

2-Amino-6-bromobenzothiazole, 4-iodobenzoic acid methyl ester, 4-methoxyphenylacetylene were purchased from Heowns (Tianjin, China). $PdCl_2(PPh_3)_2$, CuI, PPh_3, phenylacetylene, salicylaldehyde, 2-aminothiophenol, 3-bromo-2-hydroxybenzaldehyde and 4-bromo-2-hydroxybenzaldehyde were purchased from Energy Chemical (Shanghai, China). All other materials were purchased from local commercial suppliers and were of analytical reagent grade, unless otherwise stated. Solvents were purified by using standard procedures. All reactions were monitored by thin-layer chromatography (TLC).

Instruments

^{1}H NMR and ^{13}C NMR spectra were recorded at room temperature on a Bruker 500 MHz NMR spectrometer in $CDCl_3$ using the residual protonated solvents signals as the internal references, while chemical shifts were reported in ppm and coupling constants (*J*) in Hz. High resolution mass spectra (HRMS) were recorded on a Bruker instrument using standard conditions (electrospray ionization, ESI). UV-Vis absorption spectra were recorded on a U-3310 spectrophotometer. The fluorescence emission and excitation spectra were measured in a fluorospectrophotometer model F-7000. The fluorescence quantum yield (Φ_f) was determined using quinine sulfate ($\Phi_f = 0.55$ in 0.1 M H_2SO_4) as a standard[44].

Theoretical calculations

All calculations were performed using Gaussian 09 package.[25,29] To evaluate the solvent effect, toluene was employed as the solvent

in a self-consistent reaction field (SCRF) calculation using a polarized continuum model (PCM). The ground state (S_0) and the first singlet excited state (S_1) geometries of the enol and keto tautomers of ethynyl-extended regioisomers of HBT were optimized using density functional theory (DFT) and time-dependent density functional theory (TDDFT) at the B3LYP/6-31+G(d) level, respectively.

Synthesis and characterizationSynthesis and characterization of 2-(benzo[d]thiazol-2-yl)-6-bromophenol (1)

In a 100 mL round-bottomed flask equipped with a magnetic stir bar, 2-aminothiophenol (4 mmol, 501 mg) and 3-bromo-2-hydroxy benzaldehyde (4 mmol, 992 mg) were dissolved in ethanol (30 mL). Aq. 37% HCl (12 mmol, 1 mL) was gradually added to the mixture, followed by aq. 30% H_2O_2 (24 mmol, 2.5 mL). Then, the mixture was stirred at room temperature for 30 min. 20 mL water were added to quench the reaction. The mixture was extracted with ethyl acetate three times. The organic layer was washed with brine and then dried over anhydrous Na_2SO_4. The solvent was evaporated in vacuo, and the crude reaction mixture was subjected to column chromatography (ethyl acetate/petroleum ether = 1:4) to provide the product as white solid. Yield 28% (342.9 mg). ^{1}H NMR (500 MHz, $CDCl_3$): δ = 13.70 (s, 1H), 8.02 (d, J = 8.5 Hz, 1H), 7.96 (d, J = 8.0 Hz, 1H), 7.92 (dd, J = 7.5, 1.5 Hz, 1H), 7.75 (dd, J = 7.5, 1.0 Hz, 1H), 7.60–7.56 (m, 1H), 7.51–7.47 (m, 1H), 6.80 ppm (t, J = 7.5 Hz, 1H).

Synthesis and characterization of 3′-substituted HBT derivatives 7

2-(Benzo[d]thiazol-2-yl)-6-bromophenol **1** (140 mg, 0.46 mmol) was dissolved in 0.74 mL of acetic anhydride, after which 0.37 mL of pyridine (dried over sodium) were slowly added under a nitrogen atmosphere, and the resulting mixture was stirred at room temperature for 2 h. The mixture was extracted with CH_2Cl_2 three times. The organic layer was washed with HCl 0.1 M and brine successively, then dried over anhydrous Na_2SO_4. The solvent was removed under reduced pressure to provide the acetyl-protected compound **2** quantitatively. Compound **2** was dissolved in 5 mL of anhydrous toluene, then $PdCl_2(PPh_3)_2$ (42 mg, 0.06 mmol) and triethylamine (0.65 mL) were added successively. The resulting mixture was degassed with a stream of nitrogen for 30 min before aryl alkynyl (0.45 mmol) and CuI (5.7 mg, 0.03 mmol) were added. The mixture was stirred at 90 °C overnight under a nitrogen atmosphere. After cooling down, the mixture was extracted with CH_2Cl_2 three times. The organic layer was washed with brine and then dried over anhydrous Na_2SO_4. The solvent was removed under reduced pressure, after which the crude reaction mixture was subjected to column chromatography to give acetyl-protected 3′-substituted HBT derivatives **6**. Compound **6** was dissolved in 10 mL of a mixture of MeOH/THF (50/50 v:v). Potassium carbonate (193 mg, 1.4 mmol) was added and the resulting mixture was stirred at room temperature for 1 h. The crude solution was extracted with CH_2Cl_2 three times, saturated NaCl aqueous solution and then dried over anhydrous Na_2SO_4. The solvent was evaporated in vacuo, the crude reaction mixture being subjected to column chromatography to provide the pure product.

2-(Benzo[d]thiazol-2-yl)-6-(phenylethynyl)phenol (7a). Light yellow solid, yield 61% (91.8 mg). HRMS (ESI) m/z calcd for $C_{21}H_{14}NOS^+$ $[M+H]^+$ 328.07906, found 328.07907. ^{1}H NMR (500 MHz, $CDCl_3$): δ = 13.36 (s, 1H), 8.04 (d, J = 8.0 Hz, 1H), 7.97 (d, J = 8.0 Hz, 1H), 7.75 (dd, J = 8.0, 1.5 Hz, 1H), 7.67–7.64 (m, 3H), 7.59–7.56 (m, 1H), 7.50–7.47 (m, 1H), 7.43–7.38 (m, 3H), 7.02 ppm (t, J = 8.0 Hz, 1H). ^{13}C NMR (126 MHz, $CDCl_3$): δ = 168.94, 158.73, 151.64, 136.07, 132.69, 131.80, 128.40, 128.31, 126.90, 125.84, 123.43, 122.30, 121.58, 119.26, 116.91, 113.13, 94.40, 84.96 ppm.

2-(Benzo[d]thiazol-2-yl)-6-((4-methoxyphenyl)ethynyl)phenol (7b). Light yellow solid, yield 72% (118.2 mg). HRMS (ESI) m/z calcd for $C_{22}H_{16}NO_2S^+$ $[M+H]^+$ 358.08963, found 358.08960. ^{1}H NMR (500 MHz, $CDCl_3$): δ = 13.32 (s, 1H), 8.02 (d, J = 8.5 Hz, 1H), 7.95 (d, J = 8.0 Hz, 1H), 7.71 (dd, J = 8.0, 1.5 Hz, 1H), 7.64–7.59 (m, 3H), 7.56 (t, J = 8.0 Hz, 1H), 7.47 (t, J = 7.5 Hz, 1H), 6.99 (t, J = 8.0 Hz, 1H), 6.96–6.92 (m, 2H), 3.89 ppm (s, 3H). ^{13}C NMR (126 MHz, $CDCl_3$): δ = 169.00, 159.72, 158.55, 151.63, 135.91, 133.26, 132.69, 128.08, 126.86, 125.79, 122.26, 121.57, 119.25, 116.84, 115.58, 113.99, 113.44, 94.46, 83.64, 55.33 ppm.

Methyl 4-((3-(benzo[d]thiazol-2-yl)-2-hydroxyphenyl)ethynyl)-benzoate (7c). Light yellow solid, yield 52% (92.1 mg). HRMS (ESI) m/z calcd for $C_{23}H_{16}NO_3S^+$ $[M+H]^+$ 386.08454, found 386.08456. 1H NMR (500 MHz, $CDCl_3$): δ = 13.41 (s, 1H), 8.08 (d, J = 7.5 Hz, 2H), 8.03 (d, J = 8.0 Hz, 1H), 7.96 (d, J = 8.0 Hz, 1H), 7.75 (dd, J = 8.0, 1.5 Hz, 1H), 7.71 (d, J = 8.5 Hz, 2H), 7.65 (dd, J = 7.5, 1.5 Hz, 1H), 7.59–7.55 (m, 1H), 7.50–7.46 (m, 1H), 7.02 (t, J = 8.0 Hz, 1H), 3.98 ppm (s, 3H). ^{13}C NMR (126 MHz, $CDCl_3$): δ = 168.80, 166.65, 158.90, 151.56, 136.10, 132.65, 131.66, 129.51, 128.88, 128.17, 126.94, 125.90, 122.30, 121.60, 119.32, 117.00, 112.53, 93.56, 88.10, 52.23 ppm.

Synthesis and characterization of 2-(benzo[d]thiazol-2-yl)-5-bromophenol (3)

Using 4-bromine-2-hydroxy benzaldehyde as a starting material, the procedure for 2-(benzo[d]thiazol-2-yl)-6-bromophenol **1** was adopted to synthesize 2-(benzo[d]thiazol-2-yl)-5-bromophenol **3**. White solid, yield 56% (685.8 mg). ^{1}H NMR (500 MHz, $CDCl_3$): δ = 12.76 (s, 1H), 8.03 (d, J = 8.0 Hz, 1H), 7.95 (d, J = 8.0 Hz, 1H), 7.60–7.55 (m, 2H), 7.50–7.46 (m, 1H), 7.34 (d, J = 2.0 Hz, 1H), 7.14 ppm (dd, J = 8.5, 2.0 Hz, 1H).

Synthesis and characterization of 4′-substituted HBT derivatives 8

2-(Benzo[d]thiazol-2-yl)-5-bromophenol **3** (0.15 mmol, 55 mg) was dissolved in 5 mL of anhydrous toluene, then $PdCl_2(PPh_3)_2$ (42 mg, 0.06 mmol) and triethylamine (0.65 mL) were added successively. The resulting mixture was degassed with a stream of nitrogen for 30 min before aryl alkynyl (0.45 mmol) and CuI (5.7 mg, 0.03 mmol) were added. The mixture was stirred overnight at 90 °C under a nitrogen atmosphere. After cooling down, the mixture was extracted with CH_2Cl_2 three times. The organic layer was washed with brine and then dried over anhydrous Na_2SO_4. The solvent was removed under reduced pressure then the crude reaction mixture was subjected to column chromatography to afford 4′-substituted HBT derivatives **8**.

2-(Benzo[d]thiazol-2-yl)-5-(phenylethynyl)phenol (8a). Yellow solid, yield 60% (29.4 mg). HRMS (ESI) m/z calcd for $C_{21}H_{14}NOS^+$ $[M+H]^+$ 328.07906, found 328.07907. ^{1}H NMR (500 MHz, $CDCl_3$): δ = 12.65 (s, 1H), 8.04 (d, J = 8.0 Hz, 1H), 7.96 (d, J = 8.0 Hz, 1H), 7.71 (d, J = 8.0 Hz, 1H), 7.61 (dd, J = 7.5, 2.0 Hz, 2H), 7.57 (t, J = 8.0 Hz, 1H), 7.47 (t, J = 8.0 Hz, 1H), 7.44–7.40 (m, 3H), 7.32 (d, J = 0.5 Hz, 1H), 7.16 ppm (dd, J = 8.0, 1.0 Hz, 1H). ^{13}C NMR (126 MHz, $CDCl_3$): δ = 168.68, 157.71, 151.85, 132.72, 131.82, 128.69, 128.44, 128.31, 127.52, 126.85, 125.73, 122.90, 122.84, 122.28, 121.57, 120.67, 116.77, 91.79, 88.93 ppm.

2-(Benzo[d]thiazol-2-yl)-5-((4-methoxyphenyl)ethynyl)phenol (8b). Light yellow solid, yield 53% (28.4 mg). HRMS (ESI) *m/z* calcd for $C_{22}H_{16}NO_2S^+$ $[M+H]^+$ 358.08963, found 358.08966. ^{1}H NMR (500 MHz, $CDCl_3$): δ = 12.61 (s, 1H), 8.04 (d, J = 8.0 Hz, 1H), 7.96 (d, J = 8.0 Hz, 1H), 7.70 (d, J = 8.5 Hz, 1H), 7.58–7.53 (m, 3H), 7.49–7.45 (m, 1H), 7.29 (d, J = 1.5 Hz, 1H), 7.14 (dd, J = 8.0, 1.5 Hz, 1H), 6.96–6.93 (m, 2H), 3.89 ppm (s, 3H). ^{13}C NMR (126 MHz, $CDCl_3$): δ = 168.76, 160.01, 157.71, 151.87, 133.33, 132.70, 128.29, 127.94, 126.83, 125.68, 122.70, 122.26, 121.56, 120.42, 116.49, 114.97, 114.12, 92.01, 87.78, 55.36, 29.72 ppm.

Methyl 4-((4-(benzo[d]thiazol-2-yl)-3-hydroxyphenyl)ethynyl)-benzoate (8c). Light yellow solid, yield 58% (33.5 mg). HRMS (ESI) *m/z* calcd for $C_{23}H_{16}NO_3S^+$ $[M+H]^+$ 386.08454, found 386.08450. ^{1}H NMR (500 MHz, $CDCl_3$): δ = 12.65 (s, 1H), 8.09 (d, J = 8.5 Hz, 2H), 8.05 (d, J = 7.0 Hz, 1H), 7.97 (d, J = 7.5 Hz, 1H), 7.72 (d, J = 8.0 Hz, 1H), 7.66 (d, J = 8.5 Hz, 2H), 7.57–7.55 (m, 1H), 7.50–7.46 (m, 1H), 7.33 (d, J = 1.5 Hz, 1H), 7.17 (dd, J = 8.0, 1.5 Hz, 1H), 3.98 ppm (s, 3H). ^{13}C NMR (126 MHz, $CDCl_3$): δ = 168.54, 166.52, 157.71, 151.82, 132.73, 132.49, 131.70, 129.87, 129.59, 128.37, 127.55, 126.86, 125.83, 122.89, 122.34, 121.59, 120.85, 117.18, 91.71, 90.80, 52.28 ppm.

Synthesis and characterization of 2-(6-bromobenzo[d]thiazol-2-yl)phenol 5

2-Amino-5-bromobenzenethiol **4** was synthesized according to a previously reported method.[29] Light yellow solid, yield 67% (780.3 mg). ^{1}H NMR (500 MHz, $CDCl_3$): δ = 7.52 (d, J = 2.5 Hz, 1H), 7.22 (dd, J = 8.5, 2.5 Hz, 1H), 6.66 (dd, J = 8.5, 4.5 Hz, 1H), 4.21 (s, 2H), 3.02 ppm (s, 1H). Using 2-amino-5-bromobenzenethiol **4** and salicylaldehyde as starting materials, the procedure for 2-(benzo[d]-thiazol-2-yl)-6-bromophenol **1** was adopted to synthesize **5**. White solid, yield 55% (647.5 mg). ^{1}H NMR (500 MHz, $CDCl_3$): δ = 12.30 (s, 1H), 8.09 (d, J = 2.0 Hz, 1H), 7.89 (d, J = 8.5 Hz, 1H), 7.72 (dd, J = 8.0, 1.5 Hz, 1H), 7.66 (dd, J = 8.5,2.0 Hz, 1H), 7.47–7.43 (m, 1H), 7.15 (d, J = 8.5 Hz, 1H), 7.04–6.99 ppm (m, 1H).

Synthesis and characterization of 6-substituted HBT derivatives 9

Using 2-(6-bromobenzo[d]thiazol-2-yl)phenol **5** as a starting material, the procedure for 4′-substituted HBT derivatives **8** was adopted to synthesize 6-substituted HBT derivatives **9**.

2-(6-(Phenylethynyl)benzo[d]thiazol-2-yl)phenol (9a). Yellow solid, yield 67% (32.8 mg). HRMS (ESI) *m/z* calcd for $C_{21}H_{14}NOS^+$ $[M+H]^+$ 328.07906, found 328.07904. ^{1}H NMR (500 MHz, $CDCl_3$): δ = 12.41 (s, 1H), 8.13 (s, 1H), 8.00 (d, J = 8.5 Hz, 1H), 7.75–7.69 (m, 2H), 7.62–7.60 (m, 2H), 7.47–7.39 (m, 4H), 7.16 (d, J = 8.5 Hz, 1H), 7.02 ppm (t, J = 7.5 Hz, 1H). ^{13}C NMR (126 MHz, $CDCl_3$): δ = 170.36, 158.02, 151.50, 133.08, 132.84, 131.69, 130.34, 128.57, 128.50, 128.47, 124.62, 123.01, 121.95, 120.78, 119.67, 117.99, 116.69, 90.66, 88.88 ppm.

2-(6-((4-Methoxyphenyl)ethynyl)benzo[d]thiazol-2-yl)phenol (9b). Light yellow solid, yield 59% (31.6 mg). HRMS (ESI) *m/z* calcd for $C_{22}H_{16}NO_2S^+$ $[M+H]^+$ 358.08963, found 358.08957. ^{1}H NMR (500 MHz, $CDCl_3$): δ = 12.401 (s, 1H), 8.09 (d, J = 1.5 Hz, 1H), 7.98 (d, J = 8.5 Hz, 1H), 7.73 (dd, J = 8.0, 1.5 Hz, 1H), 7.68 (dd, J = 8.5, 1.5 Hz, 1H), 7.56–7.53 (m, 2H), 7.46–7.42 (m, 1H), 7.16 (dd, J = 8.5, 0.5 Hz, 1H), 7.03–7.00 (m, 1H), 6.97–6.93 (m, 2H), 3.99 ppm (s, 3H). ^{13}C NMR (126 MHz, $CDCl_3$): δ = 170.15, 159.91, 158.00, 151.30, 134.34, 133.16, 133.02, 132.84, 130.23, 128.48, 124.38, 121.93, 121.19, 119.66, 117.97, 116.74, 115.08, 114.15, 90.76, 87.62, 55.36 ppm.

Methyl 4-((2-(2-hydroxyphenyl)benzo[d]thiazol-6-yl)ethynyl)benzoate (9c). Light yellow solid, yield 53% (30.6 mg). HRMS (ESI) *m/z* calcd for $C_{23}H_{16}NO_3S^+$ $[M+H]^+$ 386.08454, found 386.08456. ^{1}H NMR (500 MHz, $CDCl_3$): δ = 12.66 (s, 1H), 8.10–8.08 (m, 2H), 8.05 (d, J = 8.0 Hz, 1H), 7.97 (d, J = 8.0 Hz, 1H), 7.73 (d, J = 8.0 Hz, 1H), 7.68–7.65 (m, 2H), 7.60–7.56 (m, 1H), 7.50–7.46 (m, 1H), 7.33 (d, J = 1.5 Hz, 1H), 7.18 (dd, J = 8.0, 1.5 Hz, 1H), 3.99 ppm (s, 3H). ^{13}C NMR (126 MHz, $CDCl_3$): δ = 168.55, 166.52, 157.72, 151.82, 132.73, 131.71, 129.88, 129.59, 128.38, 127.55, 126.91, 126.81, 125.83, 122.90, 122.35, 121.59, 120.85, 117.19, 91.71, 90.80, 52.28, 29.72 ppm.

Acknowledgements

This study was supported by the National Natural Science Foundation of China (21405122), the Natural Science Foundation of Shaanxi (2016JM2009) and the Fundamental Research Funds for the Central Universities (2452015428).

Keywords: density functional calculations · electronic structure · excited state intramolecular proton transfer · regioisomers · solvent effects

[1] O. K. Abou-Zied, R. Jimenez, E. H. Z. Thompson, D. P. Millar, F. E. Romesberg, *J. Phys. Chem. A* **2002**, *106*, 3665–3672.
[2] S. Chai, G. J. Zhao, P. Song, S. Q. Yang, J. Y. Liu, K. L. Han, *Phys. Chem. Chem. Phys.* **2009**, *11*, 4385–4390.
[3] K. Y. Chen, C. C. Hsieh, Y. M. Cheng, C. H. Lai, P. T. Chou, *Chem. Commun.* **2006**, 4395–4397.
[4] J. Seo, A. Sehoon Kim, S. Y. Park, *J. Am. Chem. Soc.* **2004**, *126*, 11154–11155.
[5] J. Zhao, S. Ji, Y. Chen, H. Guo, P. Yang, *Phys. Chem. Chem. Phys.* **2012**, *14*, 8803–8817.
[6] G. J. Zhao, K. L. Han, *Acc. Chem. Res.* **2012**, *45*, 404–413.
[7] J. Zhao, H. Yao, J. Liu, M. R. Hoffmann, *J. Phys. Chem. A* **2015**, *119*, 681–688.
[8] W. Al-Soufi, K. H. Grellmann, B. Nickel, *Chem. Phys. Lett.* **1990**, *174*, 609–616.
[9] J. S. Stephan, K. H. Grellmann, *J. Phys. Chem.* **1995**, *99*, 10066–10068.
[10] A. Ohshima, A. Momotake, T. Arai, *J. Photochem. Photobiol. A* **2004**, *162*, 473–479.
[11] P. K. Sengupta, M. Kasha, *Chem. Phys. Lett.* **1979**, *68*, 382–385.
[12] K. Y. Law, J. Shoham, *J. Phys. Chem.* **1994**, *98*, 3114–3120.
[13] P. F. Barbara, L. E. Brus, P. M. Rentzepis, *J. Am. Chem. Soc.* **1980**, *102*, 5631–5635.
[14] M. A. Ríos, M. C. Ríos, *J. Phys. Chem. A* **1998**, *102*, 1560–1567.
[15] M. Rini, J. Dreyer, E. T. J. Nibbering, T. Elsaesser, *Chem. Phys. Lett.* **2003**, *374*, 13–19.
[16] O. F. Mohammed, S. Luber, V. S. Batista, E. T. Nibbering, *J. Phys. Chem. A* **2011**, *115*, 7550–7558.
[17] S. M. Aly, A. Usman, M. AlZayer, G. A. Hamdi, E. Alarousu, O. F. Mohammed, *J. Phys. Chem. B* **2015**, *119*, 2596–2603.
[18] D. Yao, S. Zhao, J. Guo, Z. Zhang, H. Zhang, Y. Liu, Y. Wang, *J. Mater. Chem.* **2011**, *21*, 3568.
[19] J. Cheng, D. Liu, L. Bao, K. Xu, Y. Yang, K. Han, *Chem. Asian J.* **2014**, *9*, 3215–3220.
[20] J. Ma, J. Zhao, P. Yang, D. Huang, C. Zhang, Q. Li, *Chem. Commun.* **2012**, *48*, 9720–9722.
[21] P. Yang, J. Zhao, W. Wu, X. Yu, Y. Liu, *J. Org. Chem.* **2012**, *77*, 6166–6178.
[22] W. Luo, H. Jiang, K. Zhang, W. Liu, X. Tang, W. Dou, Z. Ju, Z. Li, W. Liu, *J. Mater. Chem. B* **2015**, *3*, 3459–3464.
[23] Z. Huang, S. Ding, D. Yu, F. Huang, G. Feng, *Chem. Commun.* **2014**, *50*, 9185–9187.
[24] Y. Jiang, Q. Wu, X. Chang, *Talanta* **2014**, *121*, 122–126.
[25] X. Zhang, J.-Y. Liu, *Dyes Pigm.* **2016**, *125*, 80–88.

[26] T. I. Kim, H. J. Kang, G. Han, S. J. Chung, Y. Kim, *Chem. Commun.* **2009**, 5895 – 5897.
[27] J. Massue, D. Frath, P. Retailleau, G. Ulrich, R. Ziessel, *Chemistry* **2013**, *19*, 5375 – 5386.
[28] A. A. Tanpure, S. G. Srivatsan, *ChemBioChem* **2014**, *15*, 1309 – 1316.
[29] L. F. Xu, Q. Wang, Y. R. Zhang, *Dyes Pigm.* **2017**, *136*, 732 – 741.
[30] R. D. Stephens, C. E. Castro, *J. Org. Chem.* **1963**, *28*, 3313 – 3315.
[31] Y. Y. Sun, J. H. Liao, J. M. Fang, P. T. Chou, C. H. Shen, C. W. Hsu, L. C. Chen, *Org. Lett.* **2006**, *8*, 3713 – 3716.
[32] M. C. Cui, Z. J. Li, R. K. Tang, B. L. Liu, *Bioorg. Med. Chem.* **2010**, *18*, 2777 – 2784.
[33] P. Majumdar, J. Zhao, *J. Phys. Chem. B* **2015**, *119*, 2384 – 2394.
[34] M. Forés, D. A. Miquel, M. Solà, M. Orozco, F. J. Luque, *J. Phys. Chem. A* **1999**, *103*, 4525 – 4532.
[35] T. Iijima, A. Momotake, Y. Shinohara, T. Sato, Y. Nishimura, T. Arai, *J. Phys. Chem. A* **2010**, *114*, 1603 – 1609.
[36] F. S. Rodembusch, F. P. Leusin, L. F. Campo, V. Stefani, *J. Lumin.* **2007**, *126*, 728 – 734.
[37] A. Douhal, F. Amat-Guerri, M. P. Lillo, *J. Photochem. Photobiol. A* **1994**, *78*, 127 – 138.
[38] C. Hansch, A. Leo, R. W. Taft, *Chem. Rev.* **1991**, *91*, 165 – 195.
[39] C. B. Aakeröy, K. R. Seddon, *Chem. Soc. Rev.* **1993**, *22*, 397 – 407.
[40] K. Benelhadj, W. Muzuzu, J. Massue, P. Retailleau, A. Charaf-Eddin, A. D. Laurent, D. Jacquemin, G. Ulrich, R. Ziessel, *Chemistry* **2014**, *20*, 12843 – 12857.
[41] K.-i. Sakai, S. Takahashi, A. Kobayashi, T. Akutagawa, T. Nakamura, M. Dosen, M. Kato, U. Nagashima, *Dalton Trans.* **2010**, *39*, 1989 – 1995.
[42] K. Sakai, H. Kawamura, N. Kobayashi, T. Ishikawa, C. Ikeda, T. Kikuchi, T. Akutagawa, *CrystEngComm* **2014**, *16*, 3180 – 3185.
[43] G. J. Zhao, J. Y. Liu, L. C. Zhou, K. L. Han, *J. Phys. Chem. B* **2007**, *111*, 8940 – 8945.
[44] G. J. Zhao, K. L. Han, *Biophys. J.* **2008**, *94*, 38 – 46.
[45] M. Lukeman, P. Wan, *J. Am. Chem. Soc.* **2003**, *125*, 1164 – 1165.
[46] T. Mutai, H. Sawatani, T. Shida, H. Shono, K. Araki, *J. Org. Chem.* **2013**, *78*, 2482 – 2489.
[47] K. Namba, A. Osawa, S. Ishizaka, N. Kitamura, K. Tanino, *J. Am. Chem. Soc.* **2011**, *133*, 11466 – 11469.
[48] E. Yamaguchi, F. Shibahara, T. Murai, *J. Org. Chem.* **2011**, *76*, 6146 – 6158.
[49] W. H. Melhuish, *J. Phys. Chem.* **1961**, *65*, 229 – 235.

Manuscript received: September 29, 2016
Final Article published: ■■ ▮▮, 0000

FULL PAPER

Substituent Effects

Qin Wang, Longfei Xu, Yahui Niu, Yuxiu Wang, Mao-Sen Yuan, Yanrong Zhang**

■■ – ■■

Excited State Intramolecular #ProtonTransfer in Regioisomers of HBT: Effects of the Position and Electronic Nature of Substituents

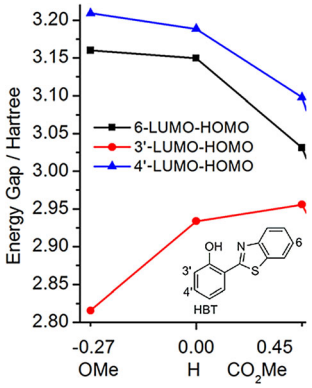

Theory and practice hand in hand: Three series of ethynyl-extended regioisomers of 2-(2′-hydroxyphenyl)benzothiazole (HBT), at the 3′-, 4′- and 6-position, respectively, have been synthesized. Changes in the absorption and emission spectra were correlated to the position and electronic nature of the substituent groups. Compared with others, 3′-substituted HBT showed red-shifted emission with smaller Φf with large σ. The theoretical calculations were in accord with the experimentally observed trends.